

This article was downloaded by:

On: 25 January 2011

Access details: *Access Details: Free Access*

Publisher *Taylor & Francis*

Informa Ltd Registered in England and Wales Registered Number: 1072954 Registered office: Mortimer House, 37-41 Mortimer Street, London W1T 3JH, UK



## Nucleosides, Nucleotides and Nucleic Acids

Publication details, including instructions for authors and subscription information:

<http://www.informaworld.com/smpp/title~content=t713597286>

### Visible-Light Photocontrol of (*E*)/(*Z*) Isomerization of the 4-(Dimethylamino)azobenzene Pseudo-Nucleotide Unit Incorporated into an Oligonucleotide and DNA Hybridization in Aqueous Media

Takashi Kamei<sup>abc</sup>; Haruhisa Akiyama<sup>b</sup>; Hisayuki Morii<sup>d</sup>; Nobuyuki Tamaoki<sup>bc</sup>; Taro Q. P. Uyeda<sup>a</sup>

<sup>a</sup> Research Institute for Cell Engineering, National Institute of Advanced Industrial Science and Technology (AIST), Ibaraki, Japan <sup>b</sup> Nanotechnology Research Institute, National Institute of Advanced Industrial Science and Technology (AIST), Ibaraki, Japan <sup>c</sup> Research Institute for Electronic Science, Hokkaido University, Hokkaido, Japan <sup>d</sup> Institute for Biological Resources and Functions, National Institute of Advanced Industrial Science and Technology (AIST), Ibaraki, Japan

Online publication date: 04 January 2011

**To cite this Article** Kamei, Takashi , Akiyama, Haruhisa , Morii, Hisayuki , Tamaoki, Nobuyuki and Uyeda, Taro Q. P.(2009) 'Visible-Light Photocontrol of (*E*)/(*Z*) Isomerization of the 4-(Dimethylamino)azobenzene Pseudo-Nucleotide Unit Incorporated into an Oligonucleotide and DNA Hybridization in Aqueous Media', *Nucleosides, Nucleotides and Nucleic Acids*, 28: 1, 12 – 28

**To link to this Article:** DOI: 10.1080/15257770802581641

**URL:** <http://dx.doi.org/10.1080/15257770802581641>

PLEASE SCROLL DOWN FOR ARTICLE

Full terms and conditions of use: <http://www.informaworld.com/terms-and-conditions-of-access.pdf>

This article may be used for research, teaching and private study purposes. Any substantial or systematic reproduction, re-distribution, re-selling, loan or sub-licensing, systematic supply or distribution in any form to anyone is expressly forbidden.

The publisher does not give any warranty express or implied or make any representation that the contents will be complete or accurate or up to date. The accuracy of any instructions, formulae and drug doses should be independently verified with primary sources. The publisher shall not be liable for any loss, actions, claims, proceedings, demand or costs or damages whatsoever or howsoever caused arising directly or indirectly in connection with or arising out of the use of this material.

## VISIBLE-LIGHT PHOTOCONTROL OF (E)/(Z) ISOMERIZATION OF THE 4-(DIMETHYLAMINO)AZOBENZENE PSEUDO-NUCLEOTIDE UNIT INCORPORATED INTO AN OLIGONUCLEOTIDE AND DNA HYBRIDIZATION IN AQUEOUS MEDIA

Takashi Kamei,<sup>1,2,3</sup> Haruhisa Akiyama,<sup>2</sup> Hisayuki Morii,<sup>4</sup>  
Nobuyuki Tamaoki,<sup>2,3</sup> and Taro Q. P. Uyeda<sup>1</sup>

<sup>1</sup>Research Institute for Cell Engineering, National Institute of Advanced Industrial Science and Technology (AIST), Ibaraki, Japan

<sup>2</sup>Nanotechnology Research Institute, National Institute of Advanced Industrial Science and Technology (AIST), Ibaraki, Japan

<sup>3</sup>Research Institute for Electronic Science, Hokkaido University, Hokkaido, Japan

<sup>4</sup>Institute for Biological Resources and Functions, National Institute of Advanced Industrial Science and Technology (AIST), Ibaraki, Japan

□ We demonstrate significant photoresponsivity in aqueous media to visible light of pseudo-oligonucleotides possessing 4-(dimethylamino)azobenzene (4-DMAzo) side chains. The spectrum of the 4-DMAzo moiety during 436 nm light irradiation at pH > 9 was clearly different from that of the all (E)-form, indicating the presence of the (Z)-form. Thermal (Z)-to-(E) recovery isomerization was faster at pH 9 ( $k_{Z\rightarrow E} = \sim 10^1 \text{ s}^{-1}$ ) than at pH 11; however, addition of 50% ethanol significantly slowed the thermal recovery isomerization at pH 9 ( $k_{Z\rightarrow E} = \sim 2 \text{ s}^{-1}$ ) and increased the magnitude of the spectral changes. Significant photoregulation of DNA hybridization by visible light was demonstrated under this condition.

**Keywords** Photoregulating DNA hybridization; photoresponsive oligonucleotides; visible light; (E)/(Z) isomerization; 4-(dimethylamino)azobenzene; aqueous media

### INTRODUCTION

Azobenzene is a widely employed photochromic system used in synthetic molecular devices that enables external control through photo-induced

Received 5 May 2008; accepted 21 October 2008.

This work was supported by the AIST Upbringing of Talent in Nanobiotechnology Course, Promotion Budget for Science and Technology (T. K. and T. U.), and a Grant-in-Aid for Science Research in a Priority Area “New Frontiers in Photochromism (No. 471) (N. T. and H. A.) from the Ministry of Education, Culture, Sports, and Technology (MEXT) of Japan.

Address correspondence to Takashi Kamei, Research Institute for Electronic Science, Hokkaido University, Kita 2/zyou-Nishi, Sapporo, Hokkaido 001-0021, Japan. E-mail: kamei-takashi@es.hokudai.ac.jp

(*E*)/(*Z*) isomerization. Azobenzene-conjugated molecules are particularly useful because their photo-physicochemical properties, especially the stability of the (*Z*)-form of azobenzene following UV-light irradiation, are little affected by the polarity of the solvent. This has enabled azobenzene to be used to create diverse photoresponsive biomolecules and molecular phototriggers that regulate biochemical reactions in highly polar aqueous solutions.<sup>[1–8]</sup> By contrast, the stability of the (*Z*)-form of 4-(dimethylamino)azobenzene (4-DMAzo), an azobenzene derivative with a single dialkylamino group, is strongly influenced by solvent polarity and protonation.<sup>[9,10]</sup> The rates of (*Z*)-to-(*E*) thermal recovery of 4-DMAzo compounds increase significantly with increases in either the polarity of the solvent or the proton concentration in the solution. This makes it difficult to photoregulate the isomerization of 4-DMAzo derivatives in polar and protic solvents, especially in aqueous solvents. Consequently, 4-DMAzo derivatives have proven less useful than the parent azobenzene for biomolecular devices that require photo-induced isomerization of the compounds in aqueous solutions.

We are nevertheless interested in the photocontrol of the conformation of 4-DMAzo-conjugated biomolecules because the photo-physicochemical properties of 4-DMAzo are distinct from those of the parent azobenzene. Azobenzene absorbs the UV light and undergoes (*E*)-to-(*Z*) photo-induced isomerization. Distinct from this, 4-DMAzo absorbs the visible light and undergoes (*E*)-to-(*Z*) photo-induced isomerization. In theory, if two azo-compounds that can be induced to undergo (*E*)-to-(*Z*) and (*Z*)-to-(*E*) photoconversions independently of one another are incorporated into a system, up to four metastable conformations of the system could be realized. But this requires development of methods to slow the (*Z*)-to-(*E*) thermal recovery and to increase the stability of the (*Z*)-form of 4-DMAzo compounds in aqueous solution.

Oligonucleotides conjugated with 4-DMAzo derivatives have been utilized as molecular beacons and probes.<sup>[11–17]</sup> Photo-induced isomerization of the 4-DMAzo moieties is not involved in those applications, however. In fact, there had been no reports of photoresponsive isomerization of 4-DMAzo moieties in synthesized oligonucleotides in aqueous solutions. This is because the rapidity of the thermal recovery in aqueous solution makes it difficult to record the spectral change accompanying photo-induced isomerization using a conventional UV/Vis spectrophotometer.<sup>[14,17,18]</sup> Stabilizing the (*Z*)-form of 4-DMAzo incorporated into oligonucleotides following irradiation would enable photo-regulation of DNA hybridization using visible light. In an analogous fashion, azobenzene-conjugated oligonucleotides have been shown to dissociate from their complementary oligonucleotides upon UV-induced (*E*)-to-(*Z*) isomerization.<sup>[19,20]</sup> Furthermore, as suggested above, oligonucleotides bearing two tethered azobenzene derivatives with different optical properties (e.g., azobenzene and 4-DMAzo)

should permit more sophisticated photoregulation of hybridization (e.g., site-selective or multi-step hybridization) triggered by irradiation at different wavelengths.

We recently demonstrated two distinct spectra for a 4-DMAzo unit incorporated into oligonucleotides that corresponded to the (*E*)- and (*Z*)-forms before and after visible light irradiation in the dehydrated and aprotic organic solvent, DMSO.<sup>[18]</sup> In addition, by using the laser flash photolysis technique and monitoring the time course of the absorbance change at one wavelength, we were able to detect the rapid (*Z*)-to-(*E*) thermal isomerization of 4-DMAzo moieties in photoresponsive oligonucleotides in aqueous solution at nearly neutral pH.<sup>[18]</sup> Still, very little is known about the photo-isomerization of 4-DMAzo tethered to oligonucleotides in different aqueous media. Such information, particularly methods to stabilize the (*Z*)-form, is essential for creating DNA devices utilizing structural changes in 4-DMAzo moieties. In this paper, we demonstrate visible light photore-sponsivity of a pseudo-oligonucleotide with a 4-DMAzo side chain recorded using a spectrophotometer under moderately basic conditions, and describe the photo-physicochemical properties of the 4-DMAzo moiety in aqueous media. Furthermore, this enabled us to demonstrate photocontrol of DNA hybridization by visible-light.

## RESULTS AND DISCUSSION

### pH Dependence of the Spectral Profiles of Photoresponsive Pseudo-Oligonucleotides with 4-DMAzo Side Chains (1) in Aqueous Solutions

Oligonucleotides containing built-in pseudo-nucleotides possessing 4-DMAzo side chains were prepared as described previously,<sup>[2,18]</sup> and the reversed phase HPLC profiles of the two compounds are shown in Figure 1 (1; 5'-AAAXAAAC-3', 2; 5'-AAAXAAAAAXAAA-3', where A and C represent adenosine and cytosine residues, and X represents the residue bearing 4-DMAzo, respectively; Scheme 1). The spectral profiles of 1, which was taken as a representative of the two compounds, were dependent on the pH in aqueous solutions (Figure 2), as were those of small 4-DMAzo derivative such as methyl red, for example, which is generally used as a pH indicator. At pH 1.1, the aqueous solution of 1 appeared purplish red ( $\lambda_{\max} = 542$  nm; hereafter, when we refer to " $\lambda_{\max}$ " for the pseudo-oligonucleotide, we are referring to the  $\lambda_{\max}$  value for the 4-DMAzo moiety in the visible region; Figure 2). The spectral profiles of 1 in the visible region changed dramatically as the pH was increased from 1.1 to 6.0, during which there was a decline in absorbance at  $\sim 550$  nm and an increase at  $\sim 460$  nm. The spectrum did not change significantly above pH  $\sim 6$  (Figure 2). As the pH was increased, the purplish red color of the 1 solution seen at pH 1.1 became

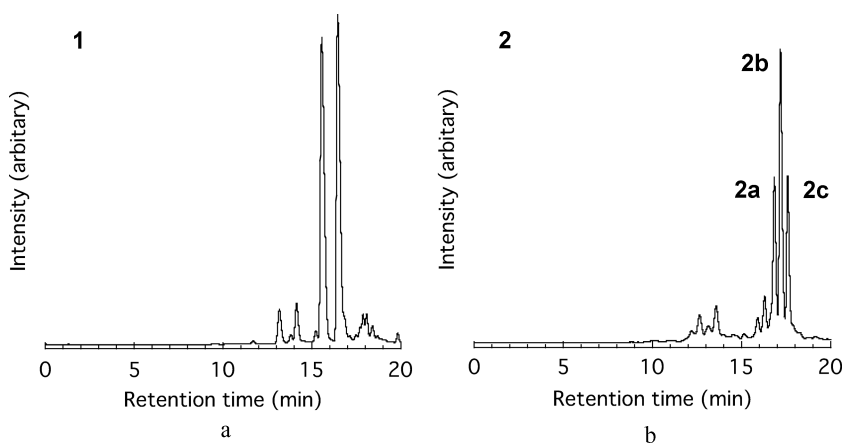
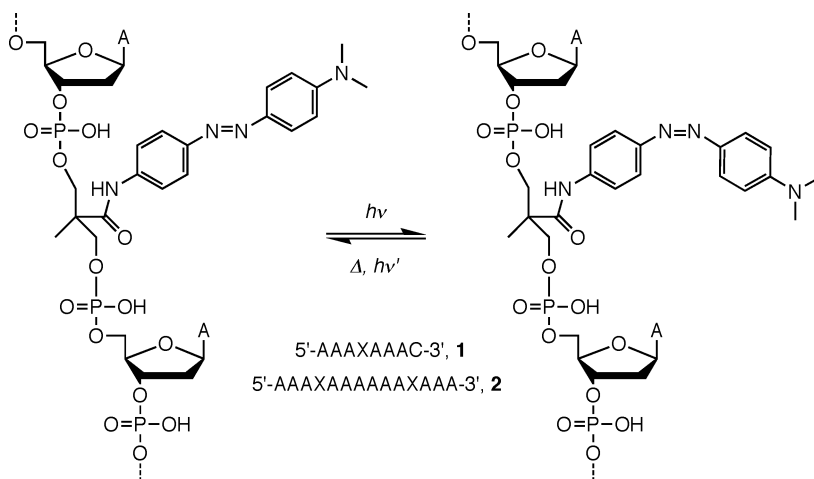


**FIGURE 1** Typical HPLC elution patterns of the photoresponsive oligonucleotides **1** (a) and **2** (b). The HPLC conditions and explanation of profiles are described in the Experimental section.

dimmer, and between pH 4.0 and 4.6, the color turned to dim yellow, which deepened as the pH was further increased to 6.0.

### Photoresponsivity of **1** to Visible Light in Basic Aqueous Solutions

Up to now, the photoresponsivity of 4-DMAzo-conjugated oligonucleotides in aqueous solution could not be measured using a conventional spectrophotometer, due to the rapidity of the thermal (*Z*)-to-(*E*) isomerization.<sup>[14,17,18]</sup> Only by using laser flash photolysis could one detect the rapid thermal (*Z*)-to-(*E*) recovery isomerization of the 4-DMAzo moiety



**SCHEME 1** Visible-light photoresponsive oligonucleotide **1** and **2** containing built-in pseudonucleotides with 4-DMAzo side chains. Reversible (*E*) (left)/(*Z*) (right) isomerization of the 4-DMAzo moiety (pseudo residue X) in the photoresponsive oligonucleotides in aqueous solution.

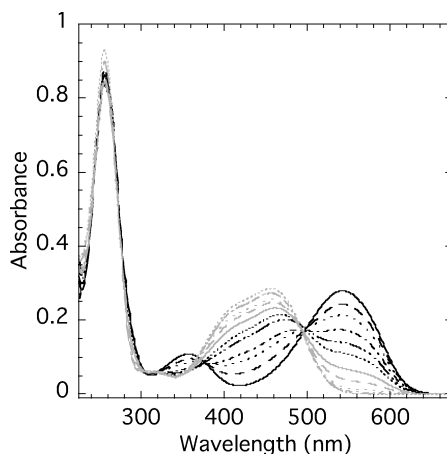


**FIGURE 2** pH dependence of the absorption spectral profiles of **1** in buffers at various pHs: concentration of **1**, 8.7  $\mu\text{M}$ ; temperature, 22~23°C. The pH values were 1.1, 2.0, 2.5, 3.0, 3.6, 4.0, 4.6, 5.1, 5.5, 6.0, 7.1 and 8.1. With increasing pH, there were increases in absorbance at around 450 nm and decreases at around 550 nm. The buffers used were hydrogen chloride-potassium chloride for pH = 1.1 and 2.0, citrate-phosphate for pH = 2.5~7.1 and phosphate for pH = 8.1.

in **1** after photo-induced (*E*)-to-(*Z*) isomerization.<sup>[18]</sup> On the other hand, taking into consideration the fact that small molecule derivatives of 4-DMAzo are barely soluble in water, Sanchez and de Rossi studied the photo-physicochemical properties of these DMAzo molecules dissolved in co-solvents composed of water and organic solvents. Using this approach, they were able to slow the thermal (*Z*)-to-(*E*) isomerization of these DMAzo derivatives by adding a high concentration of NaOH or cyclodextrin, and then record their photo-induced isomerization in aqueous solutions.<sup>[10,21,22]</sup> Because **1** is readily soluble in water, we also attempted to assess the photoresponsivity of its 4-DMAzo moiety in aqueous solutions. Instead of simply adding NaOH to the solution, however, we tested the photoresponsivity of **1** in pH controlled buffers, ranging from pH 7.9 to ~12.8, in order to prevent protons that disengaged from the DNA backbone strand from acting on the pH of the aqueous solutions. In addition, we used a spectrophotometer that was modified to record spectra while simultaneously irradiating with light at a fixed wavelength across the measuring beam. This enabled us to record photo-stationary states containing the (*Z*)-form 4-DMAzo moieties, even in moderately basic aqueous buffers, where the (*Z*)-to-(*E*) thermal recovery would be expected to be too rapid to evaluate photoresponsivity with a conventional spectrophotometer.

Figure 3 shows the changes in the spectral profiles of the 4-DMAzo moiety tethered to **1** in aqueous solutions before (gray solid lines), during (black solid lines), and after (dotted or, dotted and dashed lines) irradiation with 436 nm light at several pHs. In this basic pH region, the six spectral profiles of **1** resembled one another prior to irradiation and showed similar

$\lambda_{\max}$  ( $= 462\sim 464$  nm) and half-bandwidth ( $= 5940\sim 6438$  cm $^{-1}$ ) values. During visible light ( $\lambda = 436$  nm) irradiation in buffers above pH  $\approx 9$ , the spectral profiles of **1** at the  $\pi$ - $\pi^*$  band of the photo-stationary state significantly differed from those before the irradiation (Figure 3, b–f, gray and black solid lines). Moreover, by comparing the spectra before and during irradiation (Figure 3, b–f, gray and black solid lines), we obtained clear isosbestic points ( $\lambda = 367\sim 374$  and  $521\sim 527$  nm), which remained unchanged at pHs between 9.1 and 12.8. Under our experimental conditions ( $\lambda = 436$  nm, intensity  $= \sim 17$  mW/cm $^2$  at the front of the sample cuvette), with the 4-DMAzo moieties in a photo-stationary state, the fraction comprised of the (*Z*)-form increased as pH was increased from 7.9 to 10.9 and saturated above pH 10.9. The rate constants for (*Z*)-to-(*E*) thermal recovery isomerization of the 4-DMAzo moiety, which were derived from the time course of the absorbance change at  $\lambda = 465$  nm after terminating the visible light irradiation, declined exponentially with increasing pH (Figure 4). Thus the larger fraction of 4-DMAzo moieties in the (*Z*)-form seen in more basic buffers reflects stabilization of the (*Z*)-form.

In the absence of organic solvents, Sanchez and deRossi were only able to observe significant photoresponsivity of some 4-DMAzo derivatives in aqueous solution when  $\geq 0.01$  M NaOH was added (calculated pH = 12).<sup>[10,21]</sup> By contrast, we detected significant photoresponsivity of 4-DMAzo moieties tethered to **1** at pH 9.1, thanks to a spectrophotometer that enabled continuous irradiation during measurement. Since many biological molecules are more active in the neutral pH range, the significant photoresponsivity of 4-DMAzo moieties at moderately alkaline pHs seems advantageous for use in conjunction with DNA or other biological molecules.

### Photoinduced Reversible Isomerization of **1** in Aqueous Solution

Thermal (*Z*)-to-(*E*) recovery isomerization of 4-DMAzo moieties tethered to **1** at pHs above  $\sim 12$  was slow enough that we could detect photo-induced (*Z*)-to-(*E*) isomerization after manually changing of the irradiation filter from 436 nm to 550 nm. Figure 5 shows an example recorded under strongly basic conditions (1 M NaOH). A fraction of the 4-DMAzo moieties underwent (*E*)-to-(*Z*) isomerization upon irradiation at  $\lambda = 436$  nm (Figure 5, top; trace extending from the black dotted line to the black solid line). This was followed by changing of the filter and photo-induction of (*Z*)-to-(*E*) recovery by irradiation at  $\lambda = 550$  nm (Figure 5, top; trace extending from the black solid line to the gray solid line). The extent of thermal (*Z*)-to-(*E*) recovery during the  $<1$  minute (Figure 5, top; trace extending from the black solid line to the gray dotted line) that typically elapsed between the termination of the 436 nm irradiation and the onset of the 550 nm irradiation (including the time required to change the filters)

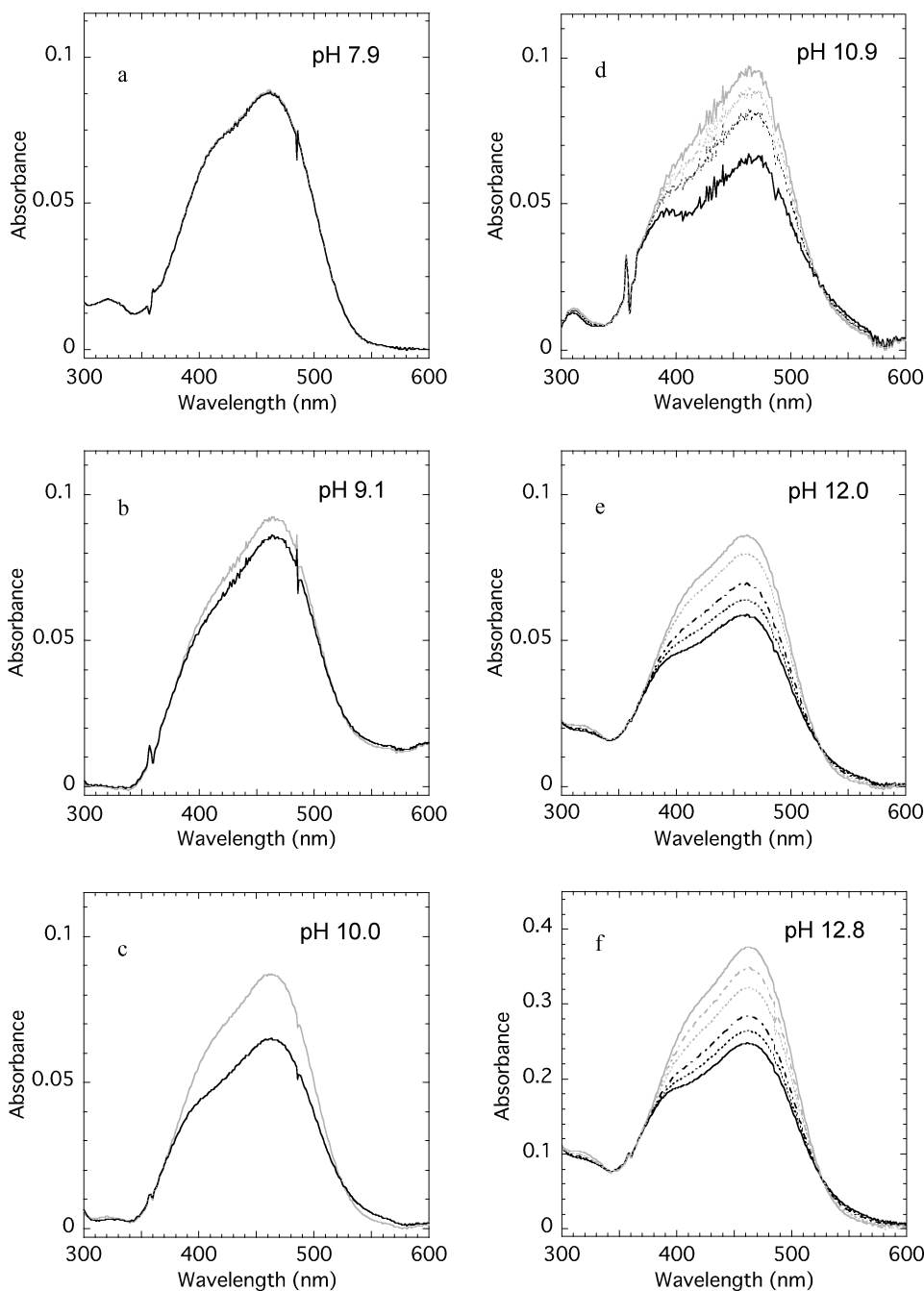


**FIGURE 3** Photoresponsive spectral profiles of **1** at the indicated pH values: temperature,  $20.0 \pm 0.1^\circ\text{C}$ . The spectral profiles of **1** before and during (photo-stationary state) visible light ( $\lambda = 436\text{ nm}$ ) irradiation are shown as solid gray and black lines, respectively. The concentrations of **1** were  $7.0\text{ }\mu\text{M}$  in the borate-citrate-phosphate buffers (a–e) and  $28\text{ }\mu\text{M}$  in the  $1\text{ M NaOH}$  aqueous solution (f). (a)–(d) Time courses of the spectral changes of **1** in the visible region. The spectra were collected at 0 s (photo-stationary state), 5 s and 15 s after irradiation and before irradiation, respectively, and show increasing absorbance at  $\sim 460\text{ nm}$ . (e) The spectra were collected 0, 1, 3 and 10 min after irradiation and before irradiation, respectively, and show increasing absorbance at  $\sim 460\text{ nm}$ . (f) The spectra were collected 0, 3, 10, 30 and 60 min after irradiation and before irradiation, respectively, and show increasing absorbance at  $\sim 460\text{ nm}$ .



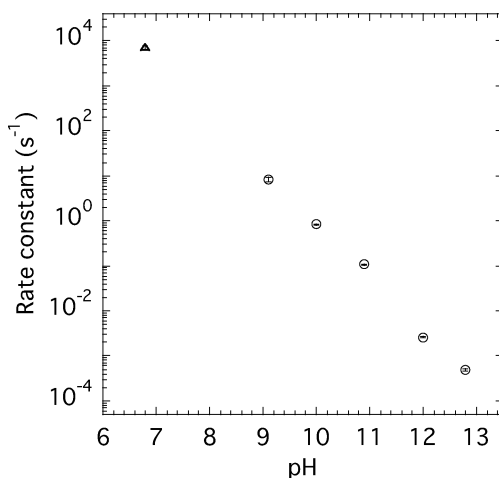


**FIGURE 4** pH dependence of the rate constant for (Z)-to-(E) thermal isomerization of 4-DMAzo moieties tethered to **1** after visible light irradiation in aqueous solution. The conditions of the aqueous solutions (compositions of buffers, concentration of **1** and temperature) were the same as in Figure 3, except for the data at pH = 6.8 (open triangles), which were adopted from our previous report, in which we used ammonium formate buffer at  $\sim 25^\circ\text{C}$ .<sup>[18]</sup> The error bars represent standard deviations ( $n = 3\sim 5$ ).

was negligible ( $< \sim 4\%$ ), given the total conversion elicited by irradiation at  $\lambda = 550$  nm. The photoresponsive properties of **1** in aqueous solution were distinct from those of oligonucleotides conjugated with parent azobenzene, in which the (E)-to-(Z) isomerization was triggered by UV light ( $300 < \lambda < 400$  nm) and (Z)-to-(E) isomerization was triggered by visible light ( $\lambda > 400$  nm).<sup>[2]</sup> In addition, there was no decay in the extent of the reversible isomerization during 10 cycles of alternating irradiation at 436 nm and 550 nm (Figure 4, bottom).

### Photoresponsivity of **1** to Visible Light in Moderately Basic Buffer Containing Ethanol

Sanchez and deRossi demonstrated that ethanol inhibited the thermal (Z)-to-(E) isomerization of *o*-methyl red, a small 4-DMAzo derivative, in strongly basic aqueous solutions (0.1 M NaOH).<sup>[10]</sup> Bearing that in mind, we next tested the effects of ethanol on the photoresponsivity of 4-DMAzo moiety tethered to **1** in histidine buffer (pH = 9; Figure 6). The pH values of the 20 mM histidine buffers used were nearly constant at pH =  $\sim 9$  in the presence of 0 to 75% ethanol (ethanol content: 0% (v/v), pH = 9.0; 25%, 9.0; 50%, 9.0; 75%, 9.1).

Before irradiation of **1** at  $\lambda = 436$  nm, increasing the ethanol concentration caused a significant blue shift in  $\lambda_{\text{max}}$  and a narrowing of the half-bandwidth at the  $\pi\text{-}\pi^*$  band (e.g.,  $\lambda_{\text{max}} = 462$  nm (0% ethanol content)  $\rightarrow$  422 nm (75%); half-bandwidth =  $6330\text{ cm}^{-1}$  (0%)  $\rightarrow$   $5740\text{ cm}^{-1}$

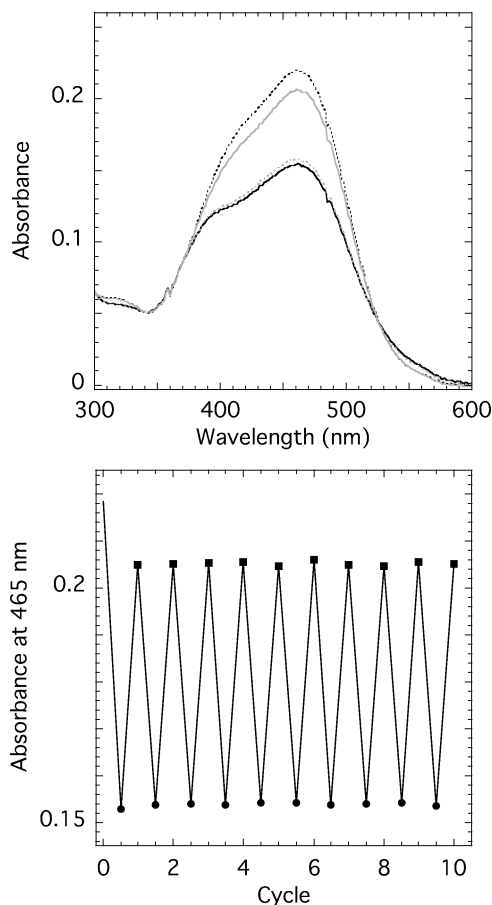


**FIGURE 5** Photo-induced reversible isomerization of **1** in 1 M NaOH aqueous solution: concentration of **1**, 16.6  $\mu\text{M}$ ; temperature,  $20.0 \pm 0.1^\circ\text{C}$ . Top: Changes in the spectral profile of the 4-DMAzo moiety tethered to **1** in the visible region before (black dotted line) and after (black solid line) irradiation at  $\lambda = 436$  nm, followed by irradiation at  $\lambda = 550$  nm (gray solid line). Thermal recovery within the time that typically elapsed between termination of the 436 nm irradiation and the onset of the 550 nm irradiation (including the time required for changing the optical filters) is shown as a gray dotted line. Bottom: Cycles of alternating reversible changes in absorbance at  $\lambda = 465$  nm corresponding to (*E*)-to-(*Z*) isomerization upon 436 nm irradiation (circles) and (*Z*)-to-(*E*) isomerization upon 550 nm irradiation (rectangles).

(75%; Figure 6, gray lines). This is consistent with our earlier finding that, for **1**, these values declined with reductions in solvent polarity.<sup>[18]</sup> The curves shown in black (Figure 6) represent the spectral profiles of **1** in the photostationary state during irradiation at  $\lambda = 436$  nm. The falling isosbestic points obtained by comparing the spectra before (Figure 6, gray lines) and during (Figure 6, black lines) irradiation were significantly blueshifted ( $\lambda = 520$  nm (0%: ethanol content)  $\rightarrow$  500 nm (75%)) as the ethanol concentration was increased. Again, this primarily reflects narrowing of the bandwidth at the  $\pi$ - $\pi^*$  band before irradiation, which is caused by the

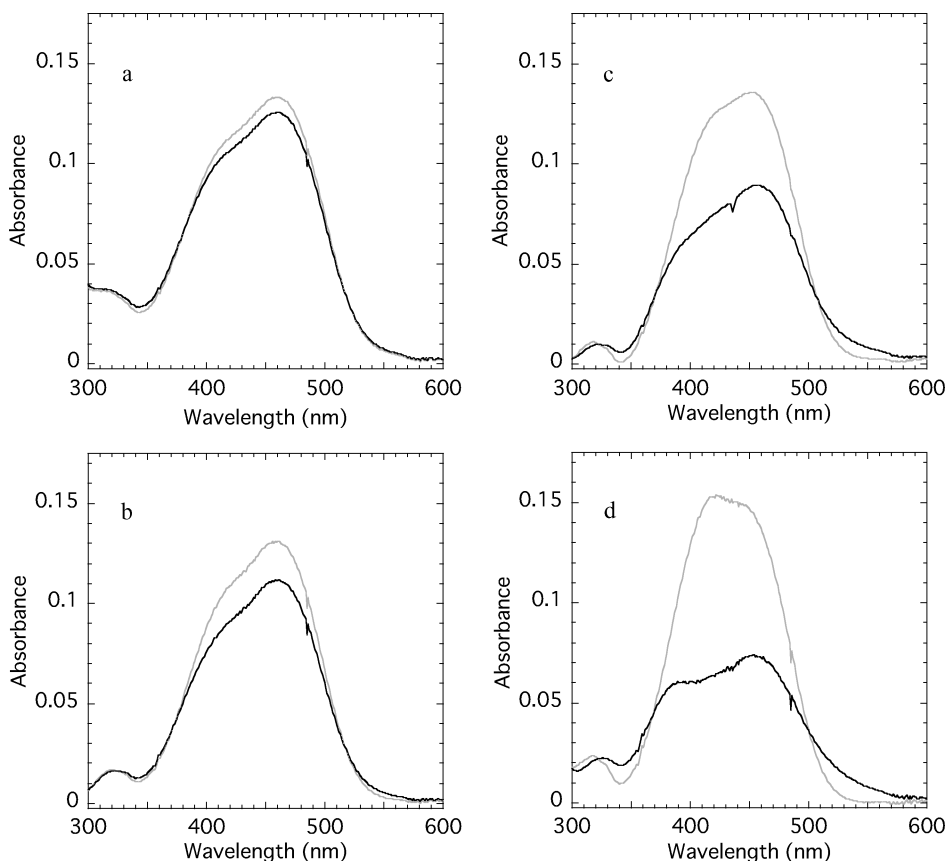


**FIGURE 6** Ethanol dependence of the photoresponsivity of **1** in moderately basic aqueous buffer: buffer, 20 mM histidine; concentration of **1**,  $\sim 10 \mu\text{M}$ ; pH =  $\sim 9$  at  $20.0 \pm 0.1^\circ\text{C}$ . (a)–(d) The spectral profiles of **1** before and during irradiation at  $\lambda = 436 \text{ nm}$  are shown as gray and black lines, respectively, (a) 0% ethanol (v/v), pH = 9.0 (b) 25%, pH = 9.0 (c) 50%, pH = 9.0 (d) 75%, pH = 9.1.

reduction in solvent polarity. Most importantly, as the ethanol concentration in the solutions was increased, the magnitudes of the changes in the spectral profile of **1** upon irradiation at  $\lambda = 436 \text{ nm}$  were enlarged (Figure 6), indicating greater increases in the (*Z*)-form fraction of the 4-DMAzo moieties in the photo-stationary state. The rate constants for the thermal (*Z*)-to-(*E*) isomerization of 4-DMAzo tethered to **1** at the four ethanol concentrations tested were estimated from the time course of the absorbance change at  $\lambda = 465 \text{ nm}$  after termination of the visible light irradiation (Figure 7). The rate constants showed an approximately exponential decline with increasing ethanol concentration, and reached  $0.7 \text{ s}^{-1}$  at 75% ethanol, which was slow enough to record significant photoresponsivity using our continuous irradiation system.

The slower thermal (*Z*)-to-(*E*) isomerization of the 4-DMAzo moiety in **1** probably reflects the more aprotic and less polar nature of ethanol, as

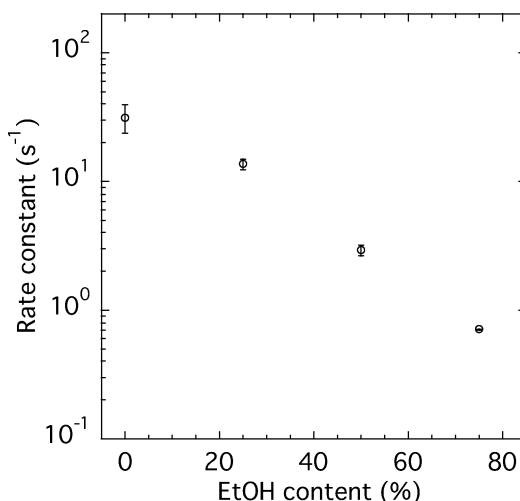


**FIGURE 7** Ethanol dependence of the rate constant for thermal (*Z*)-to-(*E*) isomerization of **1** in moderately basic aqueous buffer at pH = ~9. The experimental conditions were the same as those in Figure 6. The error bars represent standard errors of the mean ( $n = 3\sim 8$ ).

compared to water. We anticipate that mixing aqueous media with more aprotic and less polar solvents will generally stabilize the (*Z*)-form of 4-DMAzo moieties.

### Photoregulating Hybridization of DNA Duplexes through (*E*)/(*Z*) Isomerization of 4-DMAzo Moieties Tethered to the Photoresponsive Oligonucleotides (**2**) by Visible Light

Having established substantial photocontrol of structural change of 4-DMAzo moieties tethered to the photoresponsive oligonucleotides in aqueous solutions (histidine buffer in the presence of 50% ethanol controlled pH to 9.0), we next attempted to photoregulate hybridization of double-stranded DNA in an aqueous medium by visible light. To increase stability of DNA duplexes in the co-solvent of buffer and ethanol, we prepared the longer, 14 mer photoresponsive oligonucleotide **2** (Scheme 1) tethering two 4-DMAzo units. The pseudo-oligonucleotide **2** was separated to three fractions (**2a-c**) by reversed phase HPLC (for details, see the Experimental Section).

Figure 8a shows spectral profiles of a pair of **2b** and a complementary 14 mer oligonucleotide (5'-TTTTTTTTTTTTTT-3', **T14**) before visible-light irradiation at ~4°C (a gray line) and during visible-light irradiation at selected temperatures from ~4 to ~30°C (black lines) in the aqueous medium (20 mM histidine, 50% (v/v) EtOH, 250 mM NaCl, pH = 9.0). Absorption spectra were measured at 1°C ( $\pm 0.1$ ) increments and the relative absorbance at 260 nm were plotted against temperature to obtain melting

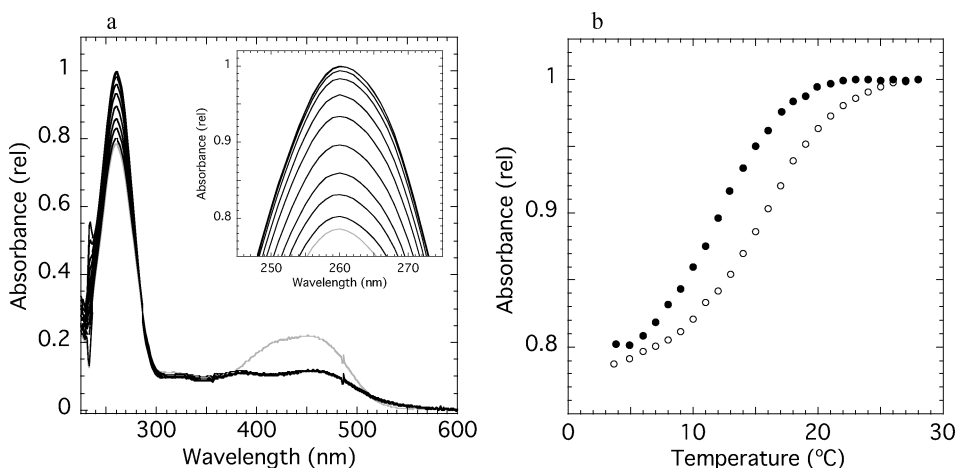


**FIGURE 8** Visible-light photoresponsivity of the duplex ( $\sim 4.8 \mu\text{M}$ ) of the pseudo-oligonucleotide (**2b** as an example) and the complementary strand (**T14**) in the aqueous medium (20 mM histidine, 50% (v/v) ethanol, 250 mM NaCl, pH = 9.0). (a) Spectral profiles of the **2b/T14** duplex without (a gray line) and during 450 nm-light irradiation (black lines). The spectra during irradiation were collected at 3.8, 8.0, 10.0, 12.0, 14.0, 16.0, 18.0, 19.9, 24.0 and 28.0°C with temperature increment during irradiation, and the increasing relative absorbance around 260 nm is magnified in the inset. (b) Melting curves of **2b/T14** duplex without (shown as dotted open circles) and upon irradiation (filled circles).

curves with or without the visible light irradiation (Figure 8b). It is known that stable double helices were formed in co-solvents comprised of water and ethanol.<sup>[23,24]</sup> By the same token, we reasoned that the pair of complementary oligonucleotides of **2** and **T14** formed duplexes in a moderately basic buffer at pH = 9.0 in the presence of 50% ethanol, judging from the hypochromicity,  $\sim 20\%$  decrease of absorbance at 260 nm at  $\sim 4^\circ\text{C}$  compared with that at  $\sim 30^\circ\text{C}$  (Figure 8). Use of a high intensity LED light source ( $\lambda = 450 \text{ nm}$ ;  $\sim 250 \text{ mW}/\text{cm}^2$ ) for visible light irradiation realized a larger fraction of the (*Z*)-form 4-DMAzo units ( $\sim 44\%$  decrease of absorbance at  $\lambda_{\text{max}}$  from that without irradiation) when compared with that obtained by irradiation with a mercury lamp ( $\sim 32\%$  decrease, as judged from the data shown in Figure 6c). This  $\sim 44\%$  decrease in absorption at  $\lambda_{\text{max}}$  was maintained over the entire temperature range tested here (Figure 8a). However, a stronger intensity ( $\sim 500 \text{ mW}/\text{cm}^2$ ) did not further induce a larger decrease in absorption at  $\lambda_{\text{max}}$  (data not shown), suggesting that the light intensity had saturated isomerization of the 4-DMAzo moieties at  $250 \text{ mW}/\text{cm}^2$ . The proportion of 4-DMAzo moiety in *Z*-form under this condition was estimated to be  $\sim 44\%$ , if the absorbance of 4-DMAzo moiety in *Z*-form at  $\lambda = \sim 455 \text{ nm}$  ( $\lambda_{\text{max}}$  of *E*-form) is 0. If 4-DMAzo moiety in *Z*-form absorbs light at 455 nm, the fraction of 4-DMAzo moiety in *Z*-form would be higher than 44%.

The melting curve of **2b/T14** duplex with visible-light irradiation obviously shifted toward the lower temperature compared to that without

**TABLE 1**  $T_m$  of the **2a-c/T14** duplex.

Duplexes	$T_{m,(Z)}$ ( $^{\circ}\text{C}$ )	$T_{m,(E)}$ ( $^{\circ}\text{C}$ )	$\Delta T_{m,\text{app}}$ ( $^{\circ}\text{C}$ )	$\Delta T_{m,\text{cor}}$ ( $^{\circ}\text{C}$ )
<b>2a/T14</b>	$13.6 \pm 0.6$	$16.5 \pm 0.4$	3.0	2.2
<b>2b/T14</b>	$13.0 \pm 1.0$	$16.1 \pm 0.6$	3.1	2.3
<b>2c/T14</b>	$13.2 \pm 0.3$	$15.3 \pm 0.3$	2.1	1.3

$T_{m,(Z)}$  and  $T_{m,(E)}$  are melting temperatures with and without visible-light irradiation, respectively.  $\Delta T_{m,\text{app}} = T_{m,(E)} - T_{m,(Z)}$ ,  $\Delta T_{m,\text{cor}} = \Delta T_{m,\text{app}} - 0.8^{\circ}\text{C}$  (see the Experimental Section for details of this correction).

irradiation (Figure 8b). Duplexes of **2a/T14** and **2c/T14**, also showed similar lowering of  $T_m$  values accompanying visible-light irradiation (Table 1). In summary, we realized photoregulation of DNA hybridization by visible-light, so that the (Z)-form of 4-DMAzo moieties tethered to a pseudo-oligonucleotide induced destabilization, that is, lowering of  $T_m$ , of the DNA duplex.

## CONCLUSIONS

We have demonstrated substantial photo-control of the conformation of oligonucleotides incorporating 4-DMAzo units—an azobenzene derivative containing a dimethylamino group—and realized photoregulation of DNA hybridization by visible light in aqueous media. Use of 4-DMAzo derivatives would realize photoregulation by visible light of biomolecules, as well as water-soluble synthetic polymers, that have been conjugated with authentic azobenzene for photocontrol by UV light.<sup>[25–30]</sup> Furthermore, combination of the DMAzo derivatives and the parent azobenzene derivatives or other photochromic molecules<sup>[31,32]</sup> with different optical properties would enable multiplex photoregulation required to create highly functional DNA devices.<sup>[33]</sup>

## EXPERIMENTAL

**General.** All reagents obtained from commercial sources were used without further purification. Highly purified water—that is, ion-exchanged RO-water ( $\geq 18.2 \text{ M}\Omega\cdot\text{cm}$ ; NANO Pure DIamond, Barnstead, IA, USA)—was used for preparing pH controlled buffers. All procedures for UV/Vis spectroscopy measurements were performed in a dark room.

**Photoresponsive Oligonucleotide (1) and (2).** The photoresponsive oligonucleotide **1** and **2** were prepared as described previously,<sup>[18]</sup> except that incorporation of 4-DMAzo using an automated synthesizer was outsourced (Gene World, Tokyo, Japan). The crude products of **1** and **2** were purified by reversed phase HPLC purification (a Symmetry C18 column (Waters, MA, USA); linear gradient acetonitrile/water (50 mM ammonium

formate) from 5/95 to 45/55 for 50 min; 1 mL/min).<sup>[18]</sup> Two major peaks corresponding to stereoisomers were observed at  $\sim 15.5$  and  $\sim 16.5$  min during HPLC purification of **1**, after correction for the dead time volume (Figure 1a). The **1**-containing fraction with the longer retention time was used in this paper. In regard to HPLC purification of **2**, the first major peak (**2a**) was observed at ca. 17 minutes, and the second (**2b**) and third (**2c**) peaks were observed with  $\sim 24$  s intervals (Figure 1b). The ratio of the peak areas was roughly **2a:2b:2c** = 1:2:1. In theory, four species of stereoisomers of **2** should be separated into four peaks with equal areas. Presumably, two of the four stereoisomers were not separated due to similar affinities to the carrier of column, and the fraction **2b** was as a mixture of the two stereoisomers. **1** and **2** were identified by MALDI-TOF mass spectrometry (**1**: obsd.  $\sim 2524$ , calcd 2523 for 5'-AAAXAAAC-3'-H<sup>+</sup>, **2a-c**: obsd.  $\sim 4532$ , calcd. 4532 for 5'-AAAXAAAAAXAAA-3'-H<sup>+</sup>) (negative mode, HPA matrix; ABI) after HPLC purification and drying.

**UV/Vis spectroscopy 1.** The spectra of **1** in aqueous solutions shown in Figure 2 were measured with a DU800 spectrophotometer (Beckman, CA, USA). The light path length of the quartz cuvette was 1 cm. The compositions of buffers are as follows. Hydrogen chloride-potassium chloride buffer: pH = 1.1 (HCl = 97 mM, KCl = 45 mM) and pH = 2.0 (13.6 mM, 45 mM). Citrate-phosphate buffer: pH = 2.5 (citric acid = 42.3 mM, Na<sub>2</sub>HPO<sub>4</sub> = 5.4 mM), pH = 3.0 (38.0 mM, 14.0 mM), pH = 3.6 (32.3 mM, 25.4 mM), pH = 4.0 (29.1 mM, 31.9 mM), pH = 4.6 (25.2 mM, 39.5 mM), pH = 5.1 (23.0 mM, 44.1 mM), pH = 5.5 (20.5 mM, 49.1 mM), pH = 6.0 (17.7 mM, 54.5 mM) and pH = 7.1 (9 mM, 72 mM). Phosphate buffer: pH = 8.1 (45 mM). All reagents used to prepare the buffers were purchased from Wako.

**UV/Vis spectroscopy 2 (simultaneous irradiation of visible light).** The spectra of **1** in aqueous media shown in Figures 3, 5 (top), and 6 were measured using an Agilent 8453 photodiode array spectrophotometer (Hewlett Packard, CA, USA) that was modified as described below. The light paths for irradiation and measurement were modified to be orthogonal, so that the sample solution in a quartz cuvette could be irradiated while the absorption spectra were simultaneously measured (the light path lengths were 2 mm and 4 mm, respectively). The irradiation light source was a high pressure mercury lamp (Ushio, Tokyo, Japan), and after passing the light through appropriate filters and a lens, the intensities at the front of the cuvette were  $\sim 17$  and  $\sim 30$  mW/cm<sup>2</sup> at  $\lambda = 436$  nm and 550 nm, respectively, when measured with an Advantest TQ8210 optical power meter (Tokyo, Japan). Occasional, spike noise at  $\lambda = 485\sim 486$  nm was deleted from the data (Figure 3d). The compositions of the buffers utilized for obtaining data in Figures 3 and 5 (top) are as follows. Borate-citrate-phosphate buffer: pH = 7.9 (H<sub>3</sub>BO<sub>3</sub> = 81 mM, citric acid = 20.3 mM, Na<sub>3</sub>PO<sub>4</sub> = 49.5 mM), pH = 9.1 (59.7 mM, 14.9 mM, 60.1 mM), pH = 10.0 (40.2 mM, 10.0 mM, 69.9

mM), pH = 10.9 (36 mM, 9 mM, 72 mM) and pH = 12.0 (15.3 mM, 3.83 mM, 82.4 mM; for Figure 3). Sodium hydroxide aqueous solution: pH = 12.8 (NaOH = ~1M; for Figure 3 and 5 (top)). L-histidine was used to prepare the histidine buffer used to obtain the data in Figures 6 and 8. All reagents used to prepare the buffers were purchased from Wako.

**Kinetic analysis.** The rate constants for thermal (*Z*)-to-(*E*) isomerization of the tethered 4-DMAzo moieties in **1** were estimated by first-order fitting of the absorbance change at  $\lambda = 465$  nm obtained with the photodiode array UV/Vis spectrophotometer (see Experimental Section, UV/Vis spectroscopy 2). Measurements during the thermal recovery process were made at up to 0.1 s intervals, which was the temporal resolution of the spectrophotometer. The R values were >0.95 for all the data, except that obtained in the histidine buffer at pH 9.0. Under those conditions, the thermal recovery was so fast that there was usually only time enough to obtain a single data point. We therefore estimated the rate constants by calculating the apparent average recovery at 0.05 s after terminating the 436 nm irradiation. At pH = ~8, recovery was even faster, and we were unable to determine the rate constant.

**$T_m$  measurement.** The spectra of **2a-c/T14** duplexes in the aqueous medium (20 mM histidine, 50% (v/v) ethanol, 250 mM NaCl, pH = 9.0) were measured by the spectrophotometer (see Experimental Section, UV/Vis spectroscopy 2) with 1 ( $\pm 0.1$ )°C increments per 3.6 minutes (average) from ~4 to ~30°C. Expansion of ethanol with temperature increment was ignored in these experiments (~4% volume expansion estimated for this medium when the temperature was raised from ~4 to ~30°C). The temperature of the cuvette holder was controlled by the thermostat, BU150S (YAMATO, Tokyo, Japan) and was monitored by TR-52 thermometer (T&D, Matsumoto, Japan). The temperature-controlled cuvette holder containing the sealed sample cuvette was placed in a box with a flow of dry air to prevent misting over the cuvette surface. LED light (Luxeon, CA, USA) was used for visible-light ( $\lambda = 450$  nm, 250 mW/cm<sup>2</sup> measured with an optical power meter; Ophir, CO, USA) irradiation to induce isomerization of 4-DMAzo moieties. Relative absorbance values of the duplexes at 260 nm calculated from the spectra were plotted against temperature, and  $T_{m,(Z)}$  (melting temperature upon irradiation) and  $T_{m,(E)}$  (without irradiation) values were obtained by the 2 point average calculation (Table 1). The apparent  $T_m$  of the control duplex, **A14/T14** (A14; 5'-AAAAAAAAAAAAAAAA-3' without 4-DMAzo), was lower by 0.8°C when the LED light was irradiated, suggesting that illumination raised the temperature of the solution by 0.8°C. Therefore the difference,  $\Delta T_{m,app} (= T_{m,(E)} - T_{m,(Z)})$  was corrected to  $\Delta T_{m,cor} (= \Delta T_{m,app} - 0.8^\circ\text{C})$  (Table 1). The concentration of each duplex, **2a-c/T14**, was adjusted to 4.8 ( $\pm 0.6$ )  $\mu\text{M}$  and all data were acquired from two independent experiments.



## REFERENCES

1. Yamana, K.; Yoshikawa, A.; Nakano, H. Synthesis of a new photoisomerizable linker for connecting two oligonucleotide segments. *Tetrahedron Lett.* **1996**, 37, 637–640.
2. Asanuma, H.; Ito, T.; Komiyama, M. Photo-responsive oligonucleotides carrying azobenzene in the side-chains. *Tetrahedron Lett.* **1998**, 39, 9015–9018.
3. Dugave, C.; Demange, L. Cis-trans isomerization of organic molecules and biomolecules: Implications and applications. *Chem. Rev.* **2003**, 103, 2475–2532.
4. Zhang, Z.H.; Burns, D.C.; Kumita, J.R.; Smart, O.S.; Woolley, G.A. A Water-soluble azobenzene cross-linker for photocontrol of peptide conformation. *Bioconjugate Chem.*, **2003**, 14, 824–829.
5. Banghart, M.; Borges, K.; Isacoff, E.; Trauner, D.; Kramer, R.H. Light-activated ion channels for remote control of neuronal firing. *Nat. Neuroscience* **2004**, 7, 1381–1386.
6. Muramatsu, S.; Kinbara, K.; Taguchi, H.; Ishii, N.; Aida, T. Semibiological molecular machine with an implemented “and” logic gate for regulation of protein folding. *J. Am. Chem. Soc.* **2006**, 128, 3764–3769.
7. Matsuzawa, Y.; Ueki, K.; Yoshida, M.; Tamaoki, N.; Nakamura, T.; Sakai, H.; Abe, M. Assembly and photoinduced organization of mono- and oligopeptide molecules containing an azobenzene moiety. *Adv. Funct. Mater.* **2007**, 17, 1507–1514.
8. Yamada, M.D.; Nakajima, Y.; Maeda, H.; Maruta, S. Photocontrol of kinesin ATPase activity using an azobenzene derivatives. *J. Biochem.* **2007**, 142, 691–698.
9. Nishimura, N.; Sueyoshi, T.; Yamanaka, H.; Imai, E.; Yamamoto, S.; Hasegawa, S. Thermal cis-to-trans isomerization of substituted azobenzenes II. Substituent and solvent effects. *Bull. Chem. Soc. Jpn.* **1976**, 49, 1381–1387.
10. Sanchez, A.; deRossi, R.H. Strong Inhibition of cis-trans isomerization of azo compounds by hydroxide ion. *J. Org. Chem.* **1993**, 58, 2094–2096.
11. Tyagi, S.; Kramer, F.R. Molecular beacons: Probes that fluoresce upon hybridization. *Nat. Biotech.* **1996**, 14, 303–308.
12. Asanuma, H.; Shirasuka, K.; Komiyama, M. H-aggregation of methyl reds by the hybridization of DNA-dye conjugates. *Chem. Lett.* **2002**, 490–491.
13. Asanuma, H.; Shirasuka, K.; Takarada, T.; Kashida, H.; Komiyama, M. DNA-dye conjugates for controllable H<sup>\*</sup> aggregation. *J. Am. Chem. Soc.* **2003**, 125, 2217–2223.
14. Gunnlaugsson, T.; Kelly, J. M.; Nieuwenhuyzen, M.; O'Brien, A.M.K. Synthesis and characterisation of novel 3'-O- and 5'-O- modified azobenzene-thymidine phosphoramidites and their oligonucleotide conjugates as colorimeter DNA probes and FRET quenchers. *Tetrahedron Lett.* **2003**, 44, 8571–8575.
15. Kashida, H.; Asanuma, H.; Komiyama, M. Alternating hetero H aggregation of different dyes by interstrand stacking from two DNA-dye conjugates. *Angew. Chem. Int. Ed.* **2004**, 43, 6522–6525.
16. Kubota, M.; Ono, A. DNA-based aromatic zipper fastened by an aromatic stacking interaction. *Tetrahedron Lett.* **2004**, 45, 5755–5758.
17. Kashida, H.; Tanaka, M.; Baba, S.; Sakamoto, T.; Kawai, G.; Asanuma, H.; Komiyama, M. Covalent incorporation of methyl red dyes into double-stranded DNA for their ordered clustering. *Chem. Eur. J.* **2006**, 12, 777–784.
18. Kamei, T.; Kudo, M.; Akiyama, H.; Wada, M.; Nagasawa, J.; Funahashi, M.; Tamaoki, N.; Uyeda, T.Q.P. Visible-Light Photoresponsivity of a 4-(Dimethylamino)azobenzene Unit Incorporated into Single-Stranded DNA: Demonstration of a large spectral change accompanying isomerization in DMSO and detection of rapid (Z)-to-(E) isomerization in aqueous solution. *Eur. J. Org. Chem.* **2007**, 1846–1853.
19. Yamana, K.; Yoshikawa, A.; Noda, R.; Nakano, H. Synthesis and binding properties of oligonucleotides containing an azobenzene linker. *Nucleosides Nucleotides* **1998**, 17, 233–242.
20. Asanuma, H.; Ito, T.; Yoshida, T.; Liang, X.G.; Komiyama, M. Photoregulation of the formation and dissociation of a DNA duplex by using the cis-trans isomerization of azobenzene. *Angew. Chem. Int. Ed.* **1999**, 38, 2393–2395.
21. Sanchez, A.M.; deRossi, R.H. Effect of hydroxide ion on the cis-trans thermal-isomerization of azobenzene derivatives. *J. Org. Chem.* **1995**, 60, 2974–2976.
22. Sanchez, A.M.; deRossi, R.H. Effect of  $\beta$ -cyclodextrin on the thermal cis-trans isomerization of azobenzenes. *J. Org. Chem.* **1996**, 61, 3446–3451.
23. Pohl, F.M. Polymorphism of a synthetic DNA in solution. *Nature* **1976**, 260, 365–366.

24. Umehara, T.; Kuwabara, S.; Mashimo, S.; Yagihara, S. Dielectric study on hydration of B-DNA, A-DNA, and Z-DNA. *Biopolymers* **1990**, 30, 649–656.
25. Irie, M. Photoresponsive polymers. *Adv. Polym. Sci.* **1990**, 94, 27–67.
26. Akiyama, H.; Tamaoki, N. Polymers derived from N-isopropylacrylamide and azobenzene-containing acrylamides: Photoresponsive affinity to water. *J. Polym. Sci. Part A-Polym. Chem.* **2004**, 42, 5200–5214.
27. Akiyama, H.; Tamaoki, N. Synthesis and photoinduced phase transitions of poly(N-isopropylacrylamide) derivative functionalized with terminal azobenzene units. *Macromolecules* **2007**, 40, 5129–5132.
28. Su, W.; Han, K.; Luo, Y.H.; Wang, Z.; Li, Y.M.; Zhang, Q.J. Formation and photoresponsive properties of giant microvesicles assembled from azobenzene-containing amphiphilic diblock copolymers. *Macromol. Chem. Phys.* **2007**, 208, 955–963.
29. Su, W.; Luo, Y. H.; Yan, Q.; Wu, S.; Han, K.; Zhang, Q.J.; Gu, Y.Q.; Li, Y.M. Photoinduced fusion of micro-vesicles self-assembled from azobenzene-containing amphiphilic diblock copolymers. *Macromol. Rapid Commun.* **2007**, 28, 1251–1256.
30. Qi, B.; Zhao, Y. Fluorescence from an azobenzene-containing diblock copolymer micelle in solution. *Langmuir* **2007**, 23, 5746–5751.
31. Letsinger, R.L.; Wu, T. Control of excimer emission and photochemistry of stilbene units by oligonucleotide hybridization. *J. Am. Chem. Soc.* **1994**, 116, 811–812.
32. Asanuma, H.; Shirasuka, K.; Yoshida, T.; Takarada, T.; Liang, X.; Komiyama, M. Spyropyran as a regulator of DNA hybridization with reversed switching mode to that of azobenzene. *Chem. Lett.* **2001**, 108–109.
33. Hiratsuka, Y.; Kamei, T.; Yumoto, N.; Uyeda, T.Q.P. Three approaches to assembling nano-bio-machines using molecular motors. *NanoBiotechnology* **2006**, 2, 101–115.